Data Paper **DOI:** 10.15541/jim20250116

Database of Eu^{2+} and Ce^{3+} Doped Phosphors for Development of Violet-light Excited White LEDs

ZHOU Zichun[1,2], ZHANG Xiang[1,2], MING Chen[1,2], SUN Yiyang[1,2]

(1. Shanghai Institute of Ceramics, Chinese Academy of Sciences, Shanghai 201899, China; 2. Center of Materials Science and Optoelectronics Engineering, University of Chinese Academy of Sciences, Beijing 100049, China)

Abstract: Commercial phosphor-converted white LEDs (pc-WLEDs) face two inherent limitations, namely blue light hazard and low color rendering index, due to the use of blue LEDs as excitation source. To address these challenges, violet LEDs are proposed as an alternative solution. Currently, phosphors that can be efficiently excited by violet light (with wavelengths from 400 to 420 nm) remain under development still. In this study, we utilize large language models to construct a comprehensive database of Eu^{2+} and Ce^{3+} doped phosphors for discovering novel violet-excited phosphors. A total of 822 phosphor data entries, including elemental compositions, crystal structures and excitation/emission wavelengths, have been extracted and validated from 9551 research papers. Compared with Ce^{3+} doped phosphors, the Eu^{2+} are in general more suited for violet-excited phosphors, as well as red-emitting phosphors. In particular, Eu^{2+} doped nitrides and sulfides are worth of exploration for violet-excited phosphors. This database is expected to be useful in the future development of phosphors for pc-WLEDs based on artificial intelligence methods. The datasets in this article are listed in Science Data Bank at http://doi.org/10.57760/sciencedb.34314.

Key words: phosphor; violet LED; large language model; database

Since the technological breakthrough of blue light-emitting diodes (LEDs) in the 1990s[1], phosphor-converted white LEDs (pc-wLEDs) have rapidly replaced traditional lighting technologies due to their high energy efficiency, environmental friendliness, and long lifespan[2-4]. Phosphors activated by lanthanide ions (*e.g.*, Eu^{2+} and Ce^{3+}) not only exhibit excellent optical stability and color performance but also possess excellent optical tunability. Through the synergistic effects of crystal field and nephelauxetic effect, they can achieve an emission spectrum of 5d-4f transitions from ultraviolet to deep red[5-7]. Currently, commercial pc-WLEDs primarily utilize blue light chips (450 nm) to excite red and yellow phosphors[8-10]. However, this technology faces two inherent drawbacks. (1) To maintain excitation efficiency, LED chips must emit an excessive amount of blue light, resulting in a high-intensity peak around 450 nm. Studies have shown that such blue light may cause retinal photochemical damage and is associated with disruptions in circadian rhythms[11-13]. (2) Due to the lack of 400–420 nm violet light, current pc-WLEDs cannot cover the full response range of the human eye, and their color rendering index (CRI) cannot meet the high-end display and medical lighting demands[14].

To address these issues, violet LEDs, which utilize violet light chips with emission wavelengths ranging from 400 to 420 nm to excite a three-primary-color phosphor system, have been proposed as a promising solution[9]. This technology enables full-spectrum emission by exciting red, yellow and blue phosphors with violet light, offering advantages as follows. (1) Spectral Safety: the blue light is controlled and released by the phosphor, effectively mitigating the potential hazards of blue light. (2) Enhanced color rendering: the added violet light component (400–420 nm) could improve the CRI. However, the development of violet-excited phosphors faces significant challenges. The 4f-5d transitions of lanthanide ions (such as Eu^{2+} and Ce^{3+}) involve complex interactions, including crystal field splitting, electron-phonon coupling, and Jahn-Teller distortion[15-16]. Additionally, excitation-state calculations based on density functional theory (DFT) are computationally expensive due to the strong correlation

Received date: 2025-03-19; **Revised date:** 2025-04-10; **Published online:** 2025-04-27
Foundation item: National Key Research and Development Program of China (2021YFB3500501)
Biography: ZHOU Zichun (2000–), male, Master candidate. E-mail: zhouzichun22@mails.ucas.ac.cn
周子淳(2000–), 男, 硕士研究生. E-mail: zhouzichun22@mails.ucas.ac.cn
Corresponding author: SUN Yiyang, professor. E-mail: yysun@mail.sic.ac.cn
孙宜阳, 研究员. E-mail: yysun@mail.sic.ac.cn

effects in the 4f electrons of lanthanide ions[17-19], as well as spin-orbit coupling (SOC) effects, making high-throughput screening challenging.

In recent years, Graph Neural Networks (GNNs)[20] have sparked a paradigm shift in the field of materials informatics by encoding crystal structures as topological graphs with vertices and edges. GNNs can learn the structure-property relationships of materials from databases such as Materials Project[21] and Inorganic Crystal Structure Database (ICSD)[22]. The GNN architecture, represented by CGCNN, has successfully predicted key material properties such as band gaps and formation energies with accuracy approaching first-principles calculations, while significantly reducing computational time[23-25]. Training machine learning models requires large databases with extensive entries. This study employs large language models (LLMs) as an auxiliary tool to construct a comprehensive material database focused on Eu^{2+} and Ce^{3+} doped phosphors. The rationality of this approach has been validated in our previous work by a small-scale database[26] extracted from 274 research papers. This work expands the literature survey to collect and organize 14795 research papers. The construction of this database aims to provide comprehensive data support for the future study of violet-excited phosphors, thereby advancing this research field.

1 Methods

To obtain a reliable database of phosphors, this study collected and organized experimental data from published papers on phosphors, assisted by the LLMs GPT-4[27], to construct a database of luminescence properties for phosphors doped by rare earth ions Eu^{2+} and Ce^{3+}.

Furthermore, the collected phosphor data were analyzed based on their publication year and country or region of origin, as shown in Fig. 1. The temporal distribution shows a steady increase in research output over the past two decades, peaking around 2017. Geographically, the majority of publications originated from China, followed by South Korea, India, Japan, the United States and Germany, reflecting the global research landscape and varying levels of technological investment in luminescent materials. This distribution underscores the regional research strengths and evolving trends in the development of phosphors. Data mining and preprocessing include the following steps, as shown in Fig. 2: (1) obtaining relevant literature through keyword search; (2) using GPT-4 to extract chemical formulas, doping elements, and excitation/emission wavelengths; (3) matching chemical formulas with the ICSD database to obtain crystallography information files (CIFs); (4) establishing the correlation between crystal structures and excitation/emission wavelengths.

Specifically, in this study, we used "Eu^{2+} and phosphors" or "Ce^{3+} and phosphors" as keywords to search and collect relevant experimental literature in Web of Science, obtaining 8556 and 6239 papers for Eu^{2+} and Ce^{3+}, respectively. It is worthwhile to note that a simple text screening was performed on these papers to ensure that the selected literature explicitly mentioned "phosphors" and considered the rare earth ions Eu^{2+} or Ce^{3+}. After this screening, only 5469 and 4082 papers were found to contain "Eu^{2+} and phosphors" or "Ce^{3+} and phosphors". These 9551 papers were then used in later construction of our phosphor database. Nextly, this study used GPT-4 *via* prompt engineering, ensuring that the model could effectively and reliably extract key data, such as the chemical formula of compounds, doping elements, emission wavelength, and excitation wavelength. With the trained model, information from the collected experimental literature was extracted and a database was constructed.

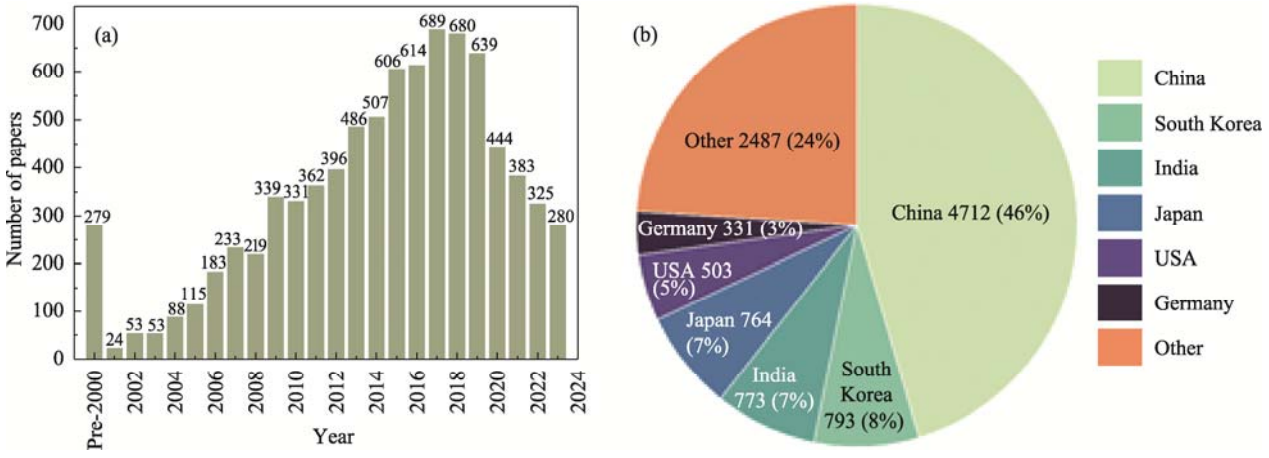

Fig. 1 Literature analysis for (a) temporal distribution and (b) geographical distribution

Colorful figures are available on website

Nextly, data cleaning and filtering were carried out on the collected data. Firstly, Python Materials Genomics (Pymatgen) package[28] was used to regularize the chemical formulas output by the trained model. For instance, there exist formula variants such as $SrMg_3SiN_4$, $Sr(Mg_3SiN_4)$, and Mg_3SrSiN_4, which differ in elemental ordering and parenthetical notation. This post-processing step ensures a unified representation of equivalent compounds. To resolve data conflicts arising from the same chemical formula, human intervention was used to select more reasonable experimental data. This step prioritized entries with complete characterization metadata such as synthesis conditions, diffraction patterns, photoluminescence (PL) spectra, photoluminescence excitation (PLE) spectra, while deprecating those exhibiting chemical inconsistencies or lacking reproducibility evidence. Subsequently, the constructed database was cross-referenced with the ICSD to obtain CIFs associated with the chemical formulas, thus identifying and filtering out compounds with fractional occupancy, as such compounds do not have well-defined crystal structures due to the randomness of site occupation. The process above ended up with 455 entries of Eu^{2+} doped and 367 entries of Ce^{3+} doped phosphors with information on their PL and PLE spectra, as well as well-defined crystal structures. Detailed information was provided in the Supporting Materials.

2 Results and discussion

We firstly carried out analysis on elemental compositions of the Eu^{2+} doped phosphor materials, as shown in Fig. 2(b). The analysis shows that oxides (57%) are the most common, followed by halides (14%) and oxyhalides (11%), whereas nitrides (8%), sulfides (6%), and nitroxides (3%) constitute comparatively minor proportions. Notably, with excitation wavelength from 400 to 420 nm, sulfides, nitroxides, and nitrides exhibit increased proportions of 33%, 41%, and 47%, respectively. In comparison, relatively small proportions of oxides (9%), halides (11%), and oxyhalides (17%) can be effectively excited by violet light.

Regarding the appearance of elements across the periodic table, it is found that alkaline earth elements dominate the cation composition (Mg^{2+}: 9%, Ca^{2+}: 15.3%, Sr^{2+}: 14.3%, Ba^{2+}: 16.3%), accounting for about 55% in total. This phenomenon may be related to the large ionic radii, which enable them to be relatively easily replaced by the rare-earth elements. Next to the alkali earth element is Si^{4+}, which may be related to the construction of a rigid lattice framework within the crystal structure. This rigid lattice framework can effectively suppress lattice vibrations, thereby reducing the probability of non-radiative transitions[29]. This result aligns with the existence of numerous silicate systems (such as Ba_2SiO_4[30], Sr_3SiO_5[31], $K_2ZrSi_3O_9$[32], and $Sr_2ZnSi_2O_7$[33]) in Eu^{2+} doped phosphors. In terms of anions, O^{2-} has the highest proportion, which is consistent with the situation that compounds containing oxygen (oxygen, oxyhalides, and nitroxides) account for 71% in the pie chart.

Similar statistics were also carried out for 367 Ce^{3+} doped phosphors. The distribution of anions and cations is similar to that of Eu^{2+} phosphors. Among cations, alkaline earth ions (Mg^{2+}: 7%, Ca^{2+}: 14.6%, Sr^{2+}: 14.4%,

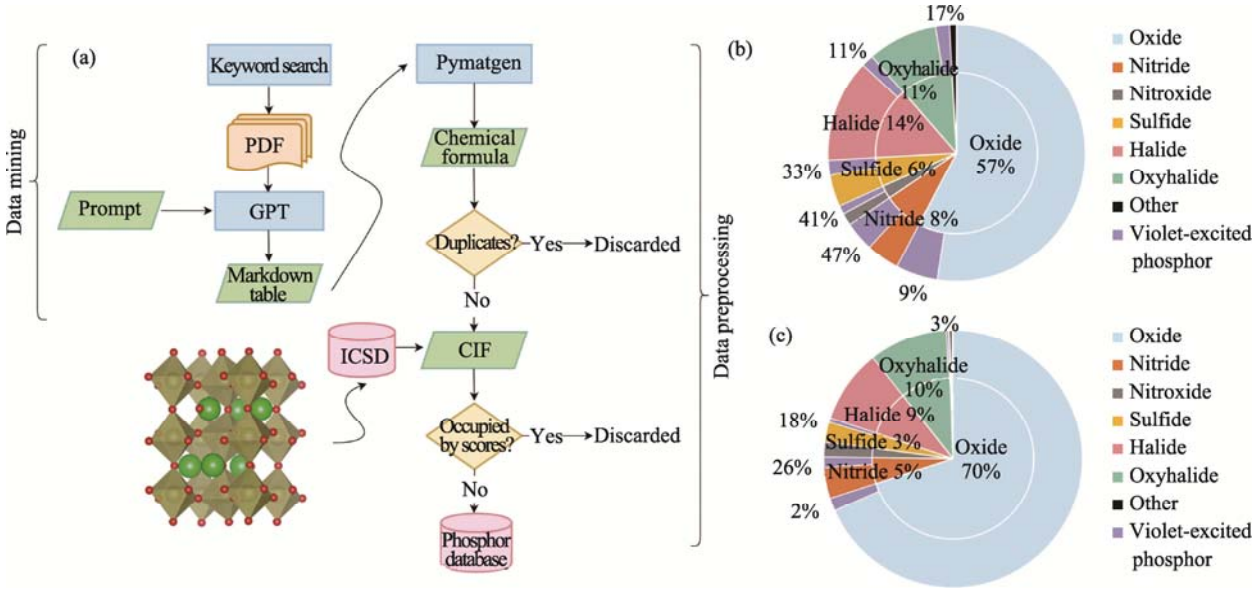

Fig. 2 Overview of data processing workflow and classification of Eu^{2+} and Ce^{3+} doped phosphors
(a) Flowchart of data mining and preprocessing; (b, c) Pie charts of compound types of (b) Eu^{2+} and (c) Ce^{3+} doped phosphors, with the outer rings also showing proportions of violet-excited phosphors in each type
Colorful figures are available on website

Ba^{2+}: 13.5%) dominate, accounting for about 50% in total, followed by Si^{4+} but with reduced proportion. For the compound types shown in Fig. 2(c), oxides, oxyhalides, halides, nitrides, sulfides and nitroxides contribute to 70%, 10%, 9%, 5%, 3% and 2%, respectively. A key difference that is worth of mentioning is that the number of violet-excited phosphors in Ce^{3+} doped materials is relatively small with only 14 compounds in our database (3.8% of total).

The statistical patterns revealed by these analyses provide guidance for the design of novel violet-excited phosphors. Firstly, Eu^{2+} doped materials are more promising as candidates for new violet-excited phosphors compared to the Ce^{3+} doped materials. Meanwhile, Eu^{2+} doped nitrides and sulfides are more likely to be excited by violet light. This insight could help for the development of violet-excited phosphors.

Fig. 3(a) illustrates the correlation between the emission and the excitation wavelengths for Eu^{2+} doped phosphors. The emission wavelengths range from 350 to 750 nm covering the full response range of the human eyes. Notably, phosphors emitting in the orange and red region (above 600 nm) are relatively rare, and nitrides are known to play an important role in this region. Nevertheless, it is worth noting that a certain number of oxides, sulfides, halides, and oxyhalides also fall into this region, suggesting that other types of phosphors may also be viable candidates for red phosphors. Therefore, in the search for red phosphors, researchers may not confine the exploration to specific compound types.

Fig. 3(b) shows the separated distribution of oxide phosphors. As an important component of phosphors, oxide phosphors are primarily concentrated within the circled region, where the excitation wavelengths range from about 300 to 400 nm and the emission wavelengths range from about 370 to 550 nm. Fig. 3(c) shows the distributions of nitrides, sulfides, halides, and oxyhalides. It is better to note that the emission wavelengths of nitrides mainly range from about 600 to 650 nm and the excitation wavelengths range from about 400 to 450 nm, with their excitation wavelengths covering the violet region. This supports their potential as violet-excited phosphor materials. Sulfides also exhibit excitation wavelengths from about 400 to 450 nm. But their relatively poor stability and thermal quenching effects at high temperatures could lead to a reduction in quantum efficiency, making it challenging to use these materials for violet-excited phosphors. Halides and oxyhalides exhibit overlapping excitation and emission ranges, with the emission wavelengths from about 400 to 450 nm and the excitation wavelengths from about 300 to 375 nm.

A main purpose of this work is to provide guidance for searching violet-excited phosphors based on all experimentally explored phosphors. Instead of using the excitation peak position as a strict requirement for defining the violet-excited phosphors, we adopted a soft condition by reviewing the PLE spectra to ensure that no potential candidates were overlooked. We used the ratio between the highest intensity in the region from 400 to 420 nm and the peak intensity of the whole PLE spectrum as the selection rule for defining phosphors as being violet-light excited. We set the ratio at 95%, and the selected phosphors are presented in Fig. 3(d), in which the horizontal axis represents the peak position in the corresponding PLE spectra. It is encouraging that the existing phosphors that can be excited by violet light already cover most of the visible region. This result suggests that the strategy of violet-light excited white LED is viable and promising.

Nextly, we analyze Ce^{3+} doped phosphors. Fig. 4(a) illustrates that, compared to Eu^{2+} doped phosphors, Ce^{3+} doped phosphors exhibit a blue shift in both excitation and emission wavelengths. As a result, there are no candidates for red phosphors, and even orange phosphors are rare. Fig. 4(b) presents the distribution of oxide phosphors. The Ce^{3+} doped oxide phosphors are primarily concentrated in the circled region, where the excitation wavelengths range from about 275 to 375 nm and the emission wavelengths range from about 300 to 450 nm. Fig. 4(c) shows the distributions of the four types of phosphors, all of which exhibit a blue shift. However, their relative positioning is similar to that of Eu^{2+} doped phosphors. Due to the overall blue shift, the number of Ce^{3+} doped phosphors that can be excited by violet light is significantly reduced, as shown in Fig. 4(d). We have marked all these compounds in the figure.

Different types of phosphors exhibit distinct advantages and limitations in terms of their luminescent properties. In the following, we analyze these phosphors by combining current knowledge with the distributions of their excitation and emission wavelengths.

Oxide phosphors are known for their excellent chemical stability[34-36], displaying high resistance to moisture and oxidation, making them suitable for applications in open or harsh environments. Their synthesis methods are well-developed, particularly the solid-state method, which offers the benefits of low cost and process simplicity, making it ideal for large-scale industrial production. However, due to the weak crystal field of oxide hosts, their capacity to modulate the energy levels of rare-earth ions is limited, thereby restricting the emission wavelength range, especially toward the longer-wavelength region. As a result, Eu^{2+} and Ce^{3+} doped oxide phosphors primarily emit within the 300–550 nm range.

In contrast, nitride phosphors exhibit superior thermal stability and oxidation resistance[37-39], with primary

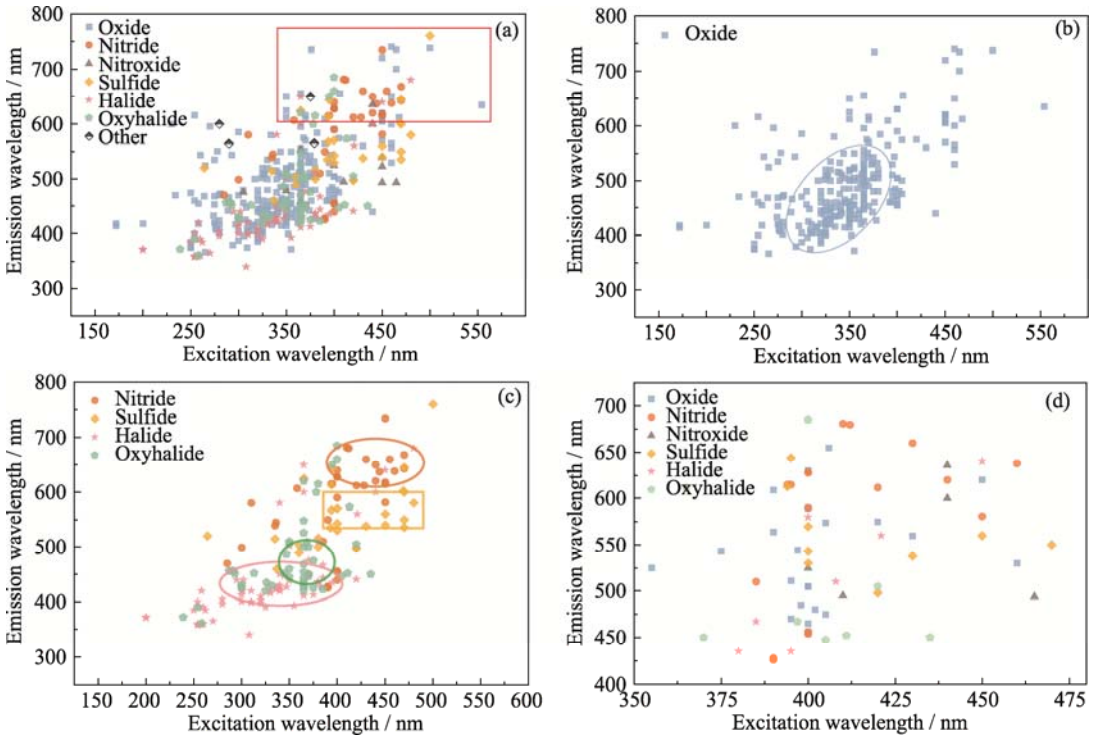

Fig. 3 Relationship between excitation and emission wavelengths of Eu^{2+} doped phosphors

(a) All compound types; (b) Oxides only; (c) Other four types; (d) Violet-excited phosphors. Note that in (d), the horizontal axis shows the peak positions of selected violet-excited phosphors based on a rule explained in the text

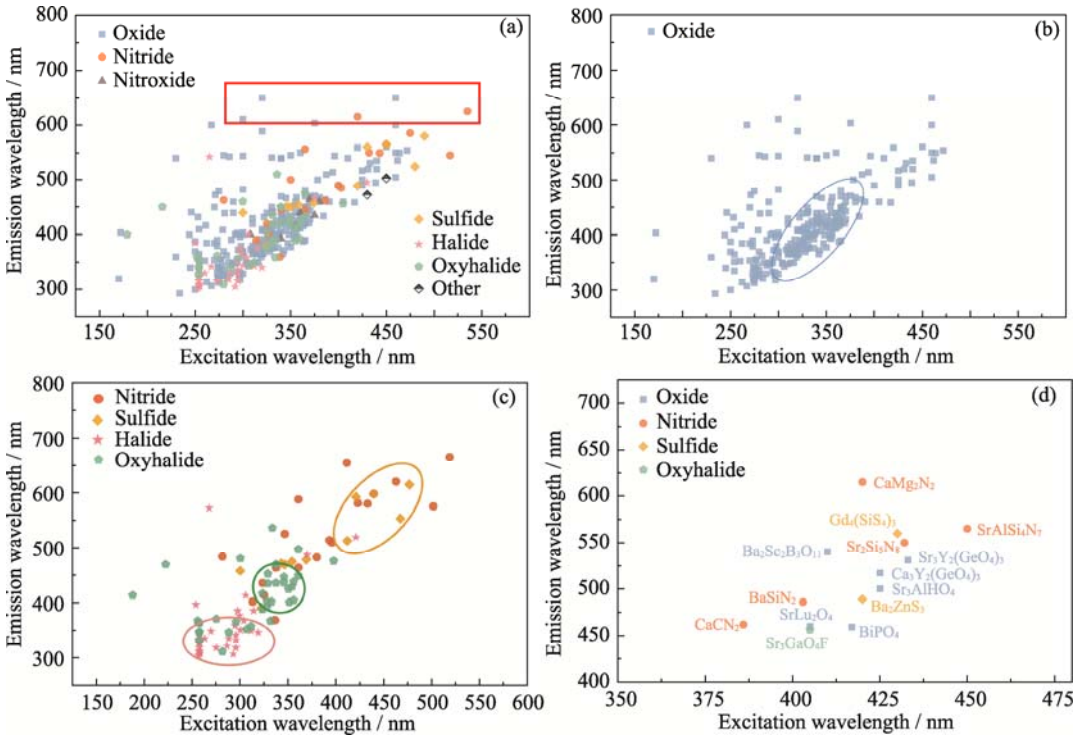

Fig. 4 Relationship between excitation and emission wavelengths of Ce^{3+} doped phosphors

(a) All compound types; (b) Oxides only; (c) Other four types; (d) Violet-excited phosphors. Note that in (d), the horizontal axis shows the peak positions of selected violet-excited phosphors based on a rule explained in the text

excitation bands ranging from 380 to 460 nm, making them suitable for a wide range of excitation sources. Theoretically, the excitation energy in Eu^{2+} and Ce^{3+} doped rare-earth systems is determined by the energy gap between the 4f and 5d electronic levels of the activator ions. Due to the shielding effect on 4f electrons by outer shells, the 4f levels are insensitive to crystal field perturbations, implying that the host lattice exerts

negligible influence on the 4f levels. Therefore, the local environment of the 5d levels mainly influences the excitation and emission behaviors. Due to the higher covalency of N^{3-} relative to O^{2-}, nitrides form stronger covalent bonds with rare-earth ions, enhancing the nephelauxetic effect and thereby shifting the energy level centroid[40]. Furthermore, nitrides often form multi-coordinated environments, inducing strong crystal field splitting of the 5d orbitals of activator ions such as Eu^{2+}, thereby lowering the transition energy of the lowest excited level and shifting the emission toward the red region[41]. Additionally, the narrower bandgap of nitride hosts provides a more favorable energy level configuration for red emission. Based on our statistical results, most phosphors are excited in the UV region (<400 nm). Given the energy-level characteristics of nitrides, they present great potential as candidates for violet-light excited phosphors. However, their synthesis typically requires high-temperature and high-pressure conditions, involving stringent process requirements and relatively high costs for raw materials and atmospheric control.

Oxynitride phosphors integrate the merits of both oxides and nitrides, offering good thermal stability and broad excitation/emission ranges. Nevertheless, their synthesis is highly sensitive to the control of the oxygen to nitrogen ratio, which results in poor consistency and relatively high production costs[42].

Sulfide phosphors also offer certain advantages in luminescence performance, particularly in achieving red and deep-red emission. Their excitation ranges usually fall within the UV to blue region, similar to that of nitrides. However, sulfide phosphors suffer from poor chemical stability, as they are prone to hydrolysis and oxidation in air, and they also exhibit limited thermal stability, with a high risk of deactivation at elevated temperatures[43]. Moreover, their synthesis often involves toxic intermediates, which impose strict requirements on the preparation and storage environments.

Halide and oxyhalide phosphors are primarily excited in the UV range (250–400 nm) and are widely used in scintillators and X-ray detectors[44-45]. However, their application in violet-light excited phosphors is limited due to incompatibility with the excitation spectrum of violet light chips.

Fig. 5 compares the wavelength distributions of Eu^{2+} and Ce^{3+} doped phosphors. We divided the wavelengths into 20-nm intervals and counted the number of phosphor materials within each interval. The histograms for excitation and emission wavelengths are presented in Figs. 5(a, b), respectively. It can be seen that, in general, the Eu^{2+} doped phosphors exhibit red-shifted excitation and emission wavelengths compared with the Ce^{3+} doped phosphors. Based on these results, Eu^{2+} doped phosphors are more probable to address the common challenges in the field of white-LED phosphors, namely, the red phosphors and violet-excited phosphors.

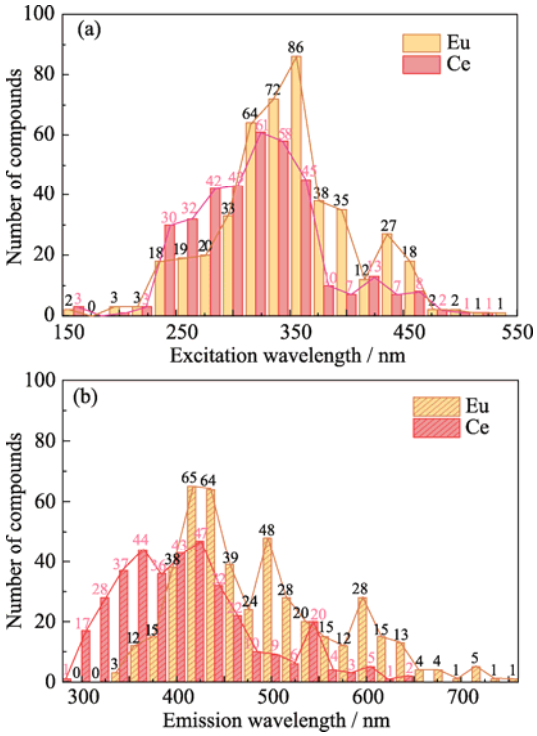

Fig. 5 Distributions of (a) excitation and (b) emission wavelengths for Eu^{2+} and Ce^{3+} doped phosphors
Colorful figures are available on website

3 Conclusions

Based on LLMs, we processed 9551 research papers on Eu^{2+} and Ce^{3+} doped phosphors with the aim of searching for novel violet-excited phosphors used in pc-WLEDs. The process extracted and validated 822 entries of phosphor data, including information on crystal structures, elemental compositions, compound types, and optical properties. With this database, some common perceptions on the phosphors, *e.g.*, alkaline earth metals (Mg^{2+}, Ca^{2+}, Sr^{2+}, and Ba^{2+}) dominate as cationic species and oxides are the most common host materials, are now backed by statistical data. To address two challenges in developing phosphors for pc-WLEDs, it was found that Ce^{3+} doped phosphors in general exhibit blue shifts on both excitation and emission wavelengths, compared to Eu^{2+} doped phosphors, making the latter more probable for discovering red phosphors and violet-excited phosphors. In particular, Eu^{2+} doped nitrides and sulfides are potential candidates for violet-light excitation. Establishing material informatics with the assistance of LLMs as practiced in this work

provides a promising approach to the discovery of novel functional materials, which could be further explored beyond the violet- excited phosphors here.

Supporting Materials

The database contains 455 entries of Eu^{2+} doped and 367 entries of Ce^{3+} doped phosphors, including their host materials' chemical formulas, ICSD collection codes, excitation wavelengths, emission wavelengths, and DOIs, which are listed in Science Data Bank at http://doi.org/10.57760/ sciencedb.34314.

References:

[1] NAKAMURA S, MUKAI T, SENOH M. High-brightness InGaN/AlGaN double-heterostructure blue-green-light-emitting diodes. *Journal of Applied Physics*, 1994, **76(12):** 8189.

[2] LI G, TIAN Y, ZHAO Y, *et al*. Recent progress in luminescence tuning of Ce^{3+} and Eu^{2+} activated phosphors for pc-WLEDs. *Chemical Society Reviews*, 2015, **44(23):** 8688.

[3] WANG L, XIE R J, SUEHIRO T, *et al*. Down-conversion nitride materials for solid state lighting: recent advances and perspectives. *Chemical Reviews*, 2018, **118(4):** 1951.

[4] GEORGE N C, DENAULT K A, SESHADRI R. Phosphors for solid-state white lighting. *Annual Review of Materials Research*, 2013, **43(1):** 481.

[5] DORENBOS P. Energy of the first $4f^7 \rightarrow 4f^6$ 5d transition of Eu^{2+} in inorganic compounds. *Journal of Luminescence*, 2003, **104(4):** 239.

[6] LAI S, ZHAO M, ZHAO Y, *et al*. Eu^{2+} doping concentration-induced site-selective occupation and photoluminescence tuning in $KSrScSi_2O_7:Eu^{2+}$ phosphor. *ACS Materials Au*, 2022, **2(3):** 374.

[7] QIN X, LIU X, HUANG W, *et al*. Lanthanide-activated phosphors based on 4f-5d optical transitions: theoretical and experimental aspects. *Chemical Reviews*, 2017, **117(5):** 4488.

[8] MUELLER-MACH R, MUELLER G O, KRAMES M R, *et al*. High-power phosphor-converted light-emitting diodes based on iii-nitrides. *IEEE Journal of Selected Topics in Quantum Electronics*, 2002, **8(2):** 339.

[9] STEIGERWALD D A, BHAT J C, COLLINS D, *et al*. Illumination with solid state lighting technology. *IEEE Journal of Selected Topics in Quantum Electronics*, 2002, **8(2):** 310.

[10] NAIR G B, SWART H C, DHOBLE S J. A review on the advancements in phosphor-converted light emitting diodes (pc-LEDs): phosphor synthesis, device fabrication and characterization. *Progress in Materials Science*, 2020, **109:** 100622.

[11] BELLIA L, BISEGNA F, SPADA G. Lighting in indoor environments: visual and non-visual effects of light sources with different spectral power distributions. *Building and Environment*, 2011, **46(10):** 1984.

[12] CAJOCHEN C, MÜNCH M, KOBIALKA S, *et al*. High sensitivity of human melatonin, alertness, thermoregulation, and heart rate to short wavelength light. *The Journal of Clinical Endocrinology & Metabolism*, 2005, **90(3):** 1311.

[13] PAULEY S M. Lighting for the human circadian clock: recent research indicates that lighting has become a public health issue. *Medical Hypotheses*, 2004, **63(4):** 588.

[14] YE S, XIAO F, PAN Y X, *et al*. Phosphors in phosphor-converted white light-emitting diodes: recent advances in materials, techniques and properties. *Materials Science and Engineering: R: Reports*, 2010, **71(1):** 1.

[15] DORENBOS P. A review on how lanthanide impurity levels change with chemistry and structure of inorganic compounds. *ECS Journal of Solid State Science and Technology*, 2013, **2(2):** R3001.

[16] WANG S, SONG Z, KONG Y, *et al*. Crystal field splitting of $4f^{n-1}5d$-levels of Ce^{3+} and Eu^{2+} in nitride compounds. *Journal of Luminescence*, 2018, **194:** 461.

[17] CHAUDHRY A, BOUTCHKO R, CHOUROU S, *et al*. First-principles study of luminescence in Eu^{2+}-doped inorganic scintillators. *Physical Review B*, 2014, **89(15):** 155105.

[18] JIA Y, MIGLIO A, PONCÉ S, *et al*. First-principles study of the luminescence of Eu^{2+}-doped phosphors. *Physical Review B*, 2017, **96(12):** 125132.

[19] JI C, CHEN Q, DUAN C K, *et al*. Rationalization of near-infrared luminescence of bismuth ions in mixed oxides. *Physical Review B*, 2024, **109(16):** 165152.

[20] GORI M, MONFARDINI G, SCARSELLI F. A new model for earning in graph domains. 2005 IEEE International Joint Conference on Neural Networks, Montreal, 2005**:** 729.

[21] JAIN A, ONG S P, HAUTIER G, *et al*. Commentary: the materials project: a materials genome approach to accelerating materials innovation. *APL Materials*, 2013, **1(1):** 011002.

[22] ZAGORAC D, MÜLLER H, RUEHL S, *et al*. Recent developments in the inorganic crystal structure database: theoretical crystal structure data and related features. *Journal of Applied Crystallography*, 2019, **52(5):** 918.

[23] XIE T, GROSSMAN J C. Crystal graph convolutional neural networks for an accurate and interpretable prediction of material properties. *Physical Review Letters*, 2018, **120(14):** 145301.

[24] CHEN C, YE W, ZUO Y, *et al*. Graph networks as a universal machine learning framework for molecules and crystals. *Chemistry of Materials*, 2019, **31(9):** 3564.

[25] LOUIS S Y, ZHAO Y, NASIRI A, *et al*. Graph convolutional neural networks with global attention for improved materials property prediction. *Physical Chemistry Chemical Physics*, 2020, **22(32):** 18141.

[26] ZHANG X, ZHOU Z, MING C, *et al*. GPT-assisted learning of structure-property relationships by graph neural networks: application to rare-earth-doped phosphors. *The Journal of Physical Chemistry Letters*, 2023, **14(50):** 11342.

[27] OPENAI, ACHIAM J, ADLER S, *et al*. GPT-4 technical report. arXiv: 2303.08774.

[28] ONG S P, RICHARDS W D, JAIN A, *et al*. Python materials genomics (pymatgen): a robust, open-source python library for materials analysis. *Computational Materials Science*, 2013, **68:** 314.

[29] BLASSE G. Thermal quenching of characteristic fluorescence. *The Journal of Chemical Physics*, 1969, **51(8):** 3529.

[30] DENAULT K A, BRGOCH J, GAULTOIS M W, *et al*. Consequences of optimal bond valence on structural rigidity and improved luminescence properties in $Sr_xBa_{2-x}SiO_4:Eu^{2+}$ orthosilicate phosphors. *Chemistry of Materials*, 2014, **26(7):** 2275.

[31] LI P, YANG Z, WANG Z, *et al*. Preparation and luminescence characteristics of $Sr_3SiO_5:Eu^{2+}$ phosphor for white LED. *Science Bulletin*, 2008, **53(7):** 974.

[32] DING X, ZHU G, GENG W, *et al*. Novel blue and green phosphors obtained from $K_2ZrSi_3O_9:Eu^{2+}$ compounds with different charge compensation ions for leds under near-UV excitation. *Journal of Materials Chemistry C*, 2015, **3(26):** 6676.

[33] YAO S, XUE L, YAN Y. Photoluminescence properties of $M_2ZnSi_2O_7$: Eu^{2+} (M=Sr, Ba). *Journal of Rare Earths*, 2010, **28:** 265.

[34] MIDGLEY C M. The crystal structure of β dicalcium silicate. *Acta*

Crystallographica, 1952, **5(3):** 307.
[35] KIM K B, KIM Y I, CHUN H G, *et al*. Structural and optical properties of $BaMgAl_{10}O_{17}:Eu^{2+}$ phosphor. *Chemistry of Materials*, 2002, **14(12):** 5045.
[36] PAN Y, WU M, SU Q. Tailored photoluminescence of YAG:Ce phosphor through various methods. *Journal of Physics and Chemistry of Solids*, 2004, **65(5):** 845.
[37] HIROSAKI N, XIE R J, KIMOTO K, *et al*. Characterization and properties of green-emitting β-SiAlON:Eu^{2+} powder phosphors for white light-emitting diodes. *Applied Physics Letters*, 2014, **86:** 211905.
[38] WATANABE H, YAMANE H, KIJIMA N. Crystal structure and luminescence of $Sr_{0.99}Eu_{0.01}AlSiN_3$. *Journal of Solid State Chemistry*, 2008, **181(8):** 1848.
[39] YANG C Y, SOM S, DAS S, *et al*. Synthesis of $Sr_2Si_5N_8:Ce^{3+}$ phosphors for white LEDs *via* efficient chemical vapor deposition. *Scientific Reports*, 2017, **7:** 45832.
[40] AULL B F, JENSSEN H P. Impact of ion-host interactions on the *5*d-to-4f spectra of lanthanide rare-earth-metal ions. I. A phenomenological crystal-field model. *Physical Review B*, 1986, **34(10):** 6640.
[41] DORENBOS P. Crystal field splitting of lanthanide $4f^{n-1}5d$-levels in inorganic compounds. *Journal of Alloys and Compounds*, 2002, **341(1/2):** 156.
[42] CHO Y, DIERRE B, SEKIGUCHI T, *et al*. Low-energy cathodoluminescence for (oxy)nitride phosphors. *Journal of Visualized Experiments*, 2016**(117):** 54249.
[43] SMET P F, MOREELS I, HENS Z, *et al*. Luminescence in sulfides: a rich history and a bright future. *Materials*, 2010, **3(4):** 2834.
[44] MARONGIU D, LAI S, LIU F, *et al*. Halide double-perovskites: high efficient light emission and beyond. *APL Energy*, 2023, **1(2):** 021501.
[45] XU L J, LIN X, HE Q, *et al*. Highly efficient eco-friendly X-ray scintillators based on an organic manganese halide. *Nature Communications*, 2020, **11:** 4329.

面向紫光激发白光 LED 的 Eu^{2+}/Ce^{3+}掺杂荧光粉数据库

周子淳[1,2], 张 翔[1,2], 明 辰[1,2], 孙宜阳[1,2]

(1. 中国科学院 上海硅酸盐研究所, 上海 201899; 2. 中国科学院大学 材料科学与光电工程中心, 北京 100049)

摘 要: 商用荧光转换白光 LED(pc-WLEDs)激发源为蓝光 LED, 这一方案存在蓝光危害和显色指数低两大固有缺陷。针对上述技术瓶颈, 学界提出了以 400~420 nm 波段紫光 LED 作为激发源的方案。然而, 能够被紫光高效激发的荧光粉目前仍处于开发阶段。为探索新型紫光激发荧光粉, 本研究基于大语言模型构建了一个 Eu^{2+}和 Ce^{3+}掺杂荧光粉的数据库。通过系统分析 9551 篇研究论文, 提取并验证了 822 组荧光粉数据, 涵盖了元素组成、晶体结构及激发/发射波长等关键参数。研究结果表明: 相比于 Ce^{3+}掺杂体系, Eu^{2+}掺杂荧光粉在紫光激发和红光发射上更具优势, 特别是氮化物和硫化物基质中的 Eu^{2+}掺杂体系, 在紫光激发上更有潜力。本工作建立的数据库为后续利用人工智能开发新型 pc-WLEDs 荧光粉提供了重要的数据支持。本文数据集可通过 https://doi.org/10.57760/sciencedb.34314 访问获取。

关 键 词: 荧光粉; 紫光 LED; 大语言模型; 数据库

中图分类号: TB34 **文献标志码:** A **文章编号:** 1000-324X(2026)03-0393-08